International Journal of Railway Research, Vol.11, No2, (2024),48-56

Iran University of Science and Technology

International Journal of

Railway Research

Condition Monitoring and Supervision of the Electric Railway 3-Phase Point Machines in Railway Signalling Systems Using the State Observer

Mohammad Ali Sandidzadeh[1*], Ahmad Mirabadi[2], Iman Sadeghi[3], Farzaad Soleymaani[4]

[1] Associate Professor, School of Railway Engineering, Iran University of Science and Technology

[2] Assistant Professor, School of Railway Engineering, Iran University of Science and Technology

[3] MSc. School of Railway Engineering, Iran University of Science and Technology

[4] Doctor of Philosophy, School of Railway Engineering, Iran University of Science and Technology

ARTICLE INFO

Article history:

Received: 05.11.2024

Accepted: 29.12.2024

Published: 08.01.2025

Keywords:

Condition monitoring,

fault detection,

electrical railway 3-phase point machine,

state observer,

Kalman filter.

A B S T R A C T

In this paper, an approach is presented to develop a condition monitoring, fault detection, and supervision system to prevent in-service failures of electrical railway 3-phase point machine mechanisms and detect slight changes in the state variables associated with some of the electric parameters of the machines. As a first step, a model of the electric point machine mechanism is discussed. In the following, state observers of the system are described, and techniques for enhanced condition monitoring are reviewed based on an analysis of the simulation of the point machine and a comparison of the data with laboratory and field test measurements. The range of failures of the point machines has been categorized into a set of basic modes. The state observer based on Kalman filter analysis allows an analysis of these modes of failure, based on the inputs and its model of system behavior and failures. The proposed method has the advantage of not requiring any equipment beyond a current sensor and the associated processing system.

1. Introduction

The mode of transport and associated systems have been experiencing fundamental transformations since about 1980. The major outwardly apparent phenomena have been the launch of high-speed lines and trains, ever increasing levels of traffic in metropolitan areas and the enforced restructuring of railway companies.

Internally, introducing the high-speed networks and increased traffic levels require that new technologies be adopted for both railway infrastructure and trains. All safety critical systems on the railway must be subject to rigorous control of performance and robust maintenance processes must be in place throughout their operational lives. Railway point machines (also known as points, depending on the railway where they are installed) are highly safety critical components of the railway. To deliver the required level of safe performance, they must operate with high precision; they have to be reliable and able to withstand the high static and dynamic loads, including impacts that result in accelerations of several hundreds.

The approach proposed in this paper has advantage of not requiring any equipment beyond a current sensor and the associated processing system while algorithms described so far require load sensors in addition to the current sensor [1-2].

The purpose of the research reported in this paper was to develop an intelligent supervision system to prevent in-service failures of railway point machine mechanisms. The approach adopted was to detect slight

*Corresponding Author
Email Address: Sandidzadeh@iust.ac.ir

changes in the state variables associated with some of the electric parameters of the machines. As a first step, a model of the electric point machine mechanism is discussed in this paper. In the following, state observers of the system are described and based on an analysis of the results of the simulation of the electric point machine and a comparison of the data with laboratory and field tests measurements, techniques for enhanced condition monitoring are reviewed. The range of failures of the point machines has been categorized into a set of basic modes. The Kalman filter analysis allows an analysis of these modes of failure, based on the inputs from the system (current, power, torque etc.) and its own model of the system behavior and failures. The Kalman Filter is a data manipulation algorithm, implemented in system software, which combines noisy measurements obtained from a dynamic system with all the other known information about that system, to obtain the best possible estimate of the variables or states of that system [3-4]. For monitoring point condition, a mathematical model of the electric point machine was developed, in state space equation form. When a fault occurs, one or several state variables of the system will be affected. Different approaches and methods for the monitoring a system's behavior, modelled as state space equations, have been introduced by researchers, for a wide range of applications [5-7]. The approach adopted by the authors is based on the observation that the loads applied to the point drive, through the point blades, follows a typical profile that is a function of the position of the blades throughout their normal or reverse movement. A full cycle of the point movement can be mapped as a time-based profile.

Given the nature of the faults and their location, i.e., recognizing the mode and type of the faults, it is possible to move beyond simply defining a threshold for each system residual. Much more data can be obtained by monitoring and analysis of the temporal behavior of each state variable, residual and/or measured parameter of the operation. For example, a fault in the mechanical transmission system can show its effect on the residuals just after its involvement in the point movement, i.e., from about 2 seconds after the start of the electric drive being switched on, while a fault in the electrical part, e.g., because of low voltage in the input, for example, may exhibits its effects immediately.

The authors use well established models to describe the behavior of critical components of points system. They begin by describing the technical components, outline the associated failure modes and then summarize the modelling approach, before presenting the results of their simulation studies. For this purpose, the authors have been provided a very straightforward system model of the induction machine. The electrical drive of the S700K electric point machine is provided by a squirrel cage three-phase induction motor, operating at the constant speed [8-11].

Assuming that the three-phase AC voltage input of the system is balanced and that the stator winding is uniformly distributed, the motor can be modelled based on well-known 2-phase equivalent motor representation, using the Park transformation, as described by the other researchers [12-14]. The non-saturated symmetrical induction motor can be described in the synchronous *d-q* frame by a set of fifth-order non-linear differential equations with respect to the rotor velocity ω , the component of rotor magnetic flux ψ_{rd}, ψ_{rq} and stator currents i_{sd}, i_{sq}.

2. Materials and Methods

In this section, electric point machine drives, fault modes of electric point drive systems, and state variable estimation using the Kalman filter are described.

2.1. Electric Point Machine Drives

Most standard point drives contain an actuating mechanism and a locking device. Drives normally also include a hand-operated crank and a selector lever to allow the power operated route setting or a local hand operation. A common arrangement is shown in Figure 1.

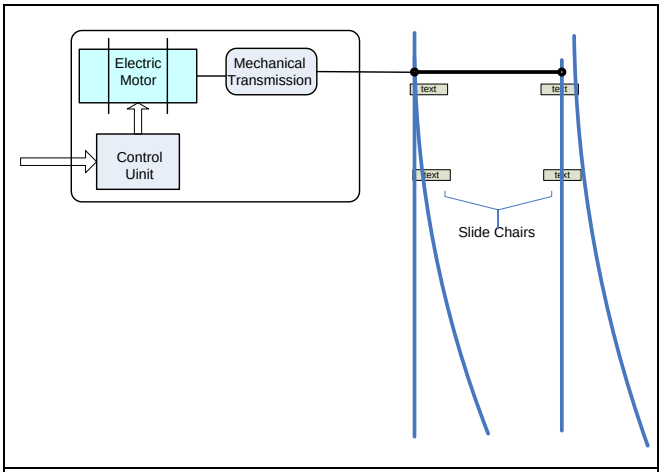

Figure 1: Electrically Operated Point Machine Mechanism

The mechanism is divided into six major subsystems:

- The motor unit which may include a contactor control arrangement and a terminal area;

- ❖ A gearbox comprising spur-gears and a worm reduction unit with overload clutch;
- ❖ The dual control mechanism;
- ❖ A controller subsystem with motor cut-off and detection contacts;
- ❖ Mechanical linkages for locking of the point
- ❖ Linkages for position detection.

The latter components are sometimes replaced with the directly operated electrical contacts. Therefore, the standard point machine is a complex electromechanical equipment with many potential failure modes.

Figure 1 shows a simplified diagram of the point drive and its linkages while a typical example of a point machine is represented in Figure 2.

The principle of operation can be readily understood from the diagrams: The motor torque is first transferred to the clutch (integral to the mechanical transmission) and then to the gearbox which changes the rotating torques into an axial direction force. The points have two directions, either pushing out (normal), or pulling in (reverse). Once the points have moved to end position, the lock mechanism engages to prevent any movement of the blades while a train passes. As mentioned, the control unit of the machine includes a detection part, which senses the orientation of the point and also checks that the movement has reached its end position. After completion of the movement, the control unit will cut off the input voltage to the motor, so that the mechanism is not subjected to unnecessary loads.

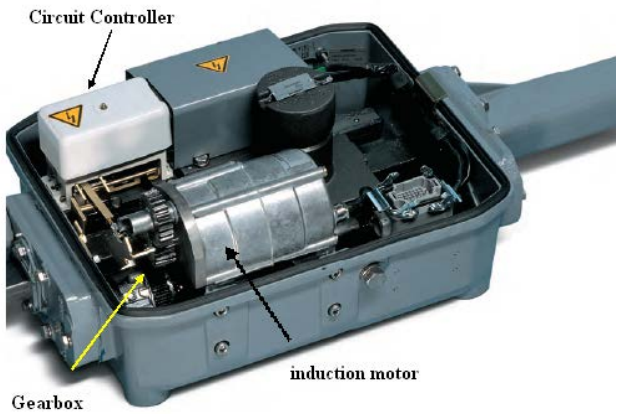

Figure 2: Electric Point Machine (S 700 K, Siemens)

The term 'point machine' is frequently used in the railway industry as an all-embracing term covering both the electrical components and the set of mechanical elements that are located in the point machine housing, effectively, the subsystems shown in Figure 2.

A complete electric drive system would normally also include the mechanical and electrical components outside the housing, e.g., the connecting linkages.

2.2. Fault Modes of Electric Point Drive Systems

As mentioned in Section 2, electric point machine drives are motor-driven devices connected to a mechanical transmission system (i.e., gearbox, clutch and mechanical linkages) which operates railway track point machines. Due to its important role in routing trains and its high safety criticality, electric point machine drives are \required to operate in a reliable, precise and safe condition. A failure analysis has been carried out to determine the most significant fault modes and to identify which parameters should be measured in a condition monitoring system.

An electrically-operated point machine (S700 K), manufactured by Siemens and widely used within the Iranian railway network, has been analysed as part of this research. The point machine faults were categorized into three types:

- ❖ Induction motor faults, that is, the stator winding faults, variations in input voltage of the point machines, aging etc.;
- ❖ Mechanical transmission faults, such as the backlash or fractured teeth in one or more of the point machine gears;
- ❖ External faults, such as the problems with the point machine blades, e.g., the point fracture, lack of lubrication, wear, extraneous objects, etc.

Table 1 summarizes the share of each of the three mentioned fault categories in causing delays to train services through point failures, for the whole of the Iranian railway network.

Table 1. Point Machine Fault Categories [5]

Fault Category	Fault and Failure	%
Mechanical fault	Overload because of extraneous objects, point fracture, dry slide chairs, point mechanism wear, and unsuitable locking arrangement	67
Transmission problem	Gear wear, gear fracture, lack of lubricant	7
Electric drive problem	Stator fault, variation of input voltage, wear of motor	26

Out of the faults listed in Table 1, dry slide chairs have the highest rate of occurrence. Dry slide chair faults are usually caused by an increase in the frictional resistance, due to a loss of lubrication and slide chair deterioration.

This type of fault causes a gradual increase in the frictional load and, consequently, results in an increase in the thrust required to move the point blades and thus, results in a higher current demand from the machine.

A timely alarm by the monitoring system, demanding lubrication and/or any required maintenance, will avoid breaks or cracks in the point machine blades and wear of the mechanism which can have further malign consequences, including derailment and need for heavy maintenance.

Figure 3 presents a complete picture of the operation of the Kalman filter and the estimation algorithm of the variable states of the system.

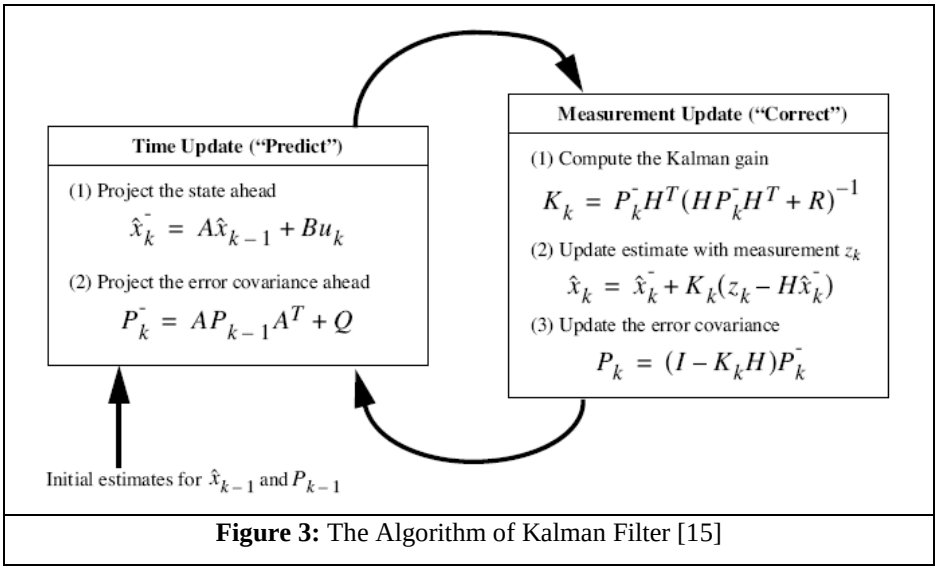

Figure 3: The Algorithm of Kalman Filter [15]

3. System Modeling

In this section, fault detection method, estimation of the state variables, and modeling of the railway three-phase AC point machine are described.

3.1. Fault Detection Method

In the research covered by this paper, a Kalman filter has been used as a state observer. By monitoring and appropriate analysis of the system state variables and related residuals by means of the state observer it is possible to detect, identify and locate faults in the point machine drive.

Although establishing simple thresholds for the state variables and residuals may assist the detection of faults and activate an alarm, this is not sufficient to identify and accurately locate faults.

Because of the wide variety of faults which may occur in a point machine, as well as the wide possible range of values associated with faults, a sophisticated analysis of the signals, states and residuals is a necessity for fault location.

The mechanism of an eelectric railway three-Phase point machine can be modelled in discrete state space equations as (1).

$$\begin{aligned} X_{n+1} &= A_n X_n + B_n U_n \\ Y_n &= C_n X_n \end{aligned} \tag{1}$$

Where X_n, the states, U_n, inputs and Y_n is outputs. Assuming that the structure and the parameters of the electric point machine mechanism are known, a state observer can be used to reconstruct the 'hidden' state variables, based on measured inputs and outputs as (2).

$$\begin{aligned} \hat{X}_k &= \hat{X}_k^- + K_k e_k \\ e_k &= (Z_k - C_k \hat{X}_k^-) \end{aligned} \tag{2}$$

Where $e_k(t)$, the residual, is the output error which acts through the observer matrix C_k on the reconstructed state vector $\hat{X}_k^-$.

3.2. Estimation of the State Variables

According to Figure 3, R and Q are positive semi-defined matrices and in general are used as non-

correlated in the time. These characteristics define the covariance matrices as (3).

The filter uses a prediction of the states X, which it compares with new measurements, by means of the measurement matrix C. The difference between the prediction and measurement residual can be used to arrive at a more accurate estimation of the states and it can also be used for the analysis of the behaviour of the system which is under study.

In this paper, the Kalman filter has been used as a state observer, through which it is possible to estimate the internal states of the system, so as to be able to detect incipient system failures.

$$P=\begin{bmatrix}10^5&0&0&0&0\\0&10^5&0&0&0\\0&0&10^5&0&0\\0&0&0&10^5&0\\0&0&0&0&10^5\end{bmatrix},$$

$$Q=\begin{bmatrix}10^{-5}&0&0&0&0\\0&10^{-5}&0&0&0\\0&0&10^{-5}&0&0\\0&0&0&10^{-5}&0\\0&0&0&0&10^{-5}\end{bmatrix}, \quad (3)$$

$$R=\begin{bmatrix}.01&0\\0&.01\end{bmatrix}$$

3.3. Modeling of the 3-Phase AC Point Machine

Restricting our discussion, for the time being, to electric 3-phase point machines as defined before, we can classify them, in a first step as electromechanical equipment, consisting of the electrical and mechanical parts.

Developing a precise mathematical model of the system requires sufficient knowledge about both the mechanical and electrical elements and also the interface between these. An overall model of the electric point machine consists of models of the induction motor and the mechanical transmission models.

The dynamic model of an induction machine, in an arbitrary *d-q* reference frame, rotating at a speed ω, can be obtained from the (4) equations, reproduced from recent works of the researchers [16-17].

$$\begin{aligned}
\frac{d}{dt}i_{sd} &= -\left(\frac{R_s}{\sigma L_s}+\frac{1-\sigma}{\sigma\tau_r}\right)i_{sd}+\omega_e i_{sq}+\frac{L_m}{\sigma L_s L_r\tau_r}\psi_{rd}\\
&\quad+\frac{L_m\omega}{\sigma L_s L_r}\psi_{rq}+\frac{1}{\sigma L_s}V_{sd}\\
\frac{d}{dt}i_{sq} &= -\omega_e i_{sd}-\left(\frac{R_s}{\sigma L_s}+\frac{1-\sigma}{\sigma\tau_r}\right)i_{sq}-\frac{L_m\omega}{\sigma L_s L_r}\psi_{rd}\\
&\quad+\frac{L_m}{\sigma L_s L_r\tau_r}\psi_{rq}+\frac{1}{\sigma L_s}V_{sq}\\
\frac{d}{dt}\psi_{rd} &= \frac{L_m}{\tau_r}i_{sd}-\frac{1}{\tau_r}\psi_{rd}+(\omega_e-\omega)\psi_{rq}\\
\frac{d}{dt}\psi_{rq} &= \frac{L_m}{\tau_r}i_{sq}-(\omega_e-\omega)\psi_{rd}-\frac{1}{\tau_r}\psi_{rq}\\
\frac{d}{dt}\omega &= \frac{3P^2L_m}{2JL_r}(i_{sq}\psi_{rd}-i_{sd}\psi_{rq})-\frac{P}{J}T_L
\end{aligned} \quad (4)$$

In these equations, ω is the angular velocity of the rotor, V_{sd} and V_{sq} are stator voltages in the synchronous *d-q* frame and T_L is the load torque.

J is the rotor's moment of inertia, P is the number of poles, R_r and R_s are rotor and stator resistances respectively, while L_r and L_s are the rotor and stator inductances, L_m is the mutual inductance, $\sigma=\left(1-L_m^2/L_S L\right)$ is the total leakage coefficient, τ_r is the rotor time constant.

The mechanical transmission system model can be obtained as (5).

$$J=J_1+\left(\frac{R_1}{R_2}\right)^2 J_2+\left(\frac{R_1}{R_2}\right)^2 J_L \quad (5)$$

The torque T_l is proportional to the amount of throwing force f and also the radius of the gear R_2. It can be modelled as (6).

$$T_l = f\times R_2 \quad (6)$$

Figure 4 represents the arrangement of the gearbox and the mechanical load.

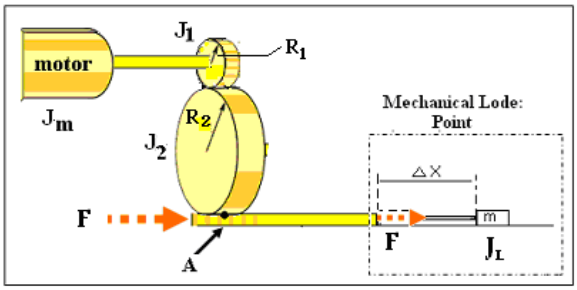

Figure 4: Gearbox Model with Mechanical Load

Returning to the state equations (1) for the electric point machine, X_n is the state variable vector containing [i_{sd}, i_{sq}, ψ_{rd}, ψ_{rq}, ω], U_n is the input vector given as [V_{sd}, V_{sq}] and Y_n the output vector as [i_{sd}, i_{sq}], as (7).

$$\begin{bmatrix} i_{sd} \\ i_{sq} \end{bmatrix}_n = \begin{bmatrix} 1 & 0 & 0 & 0 & 0 \\ 0 & 1 & 0 & 0 & 0 \end{bmatrix} \begin{bmatrix} i_{sd} \\ i_{sq} \\ \psi_{rd} \\ \psi_{rq} \\ \omega \end{bmatrix} \quad (7)$$

The researchers used a relatively simple approach to detect incipient failures in points systems, focusing on the mechanical components. They studied basic features of signals, such as peak levels and timings between peaks and troughs. The authors of the present paper, by contrast, have modelled the electrical drive of the system, identifying faults by means of filtering.

4. Results and Discussion

The authors' contribution to fault identification is in the simulation of the operation of the electric point machine and associated mechanism, using MATLAB 7.1 and the formulae described above.

The characteristics of the three-phase squirrel cage induction motor were chosen as follows: 4-pole, class A design, rated at 700 W, with a 400 V, 50 Hz three-phase supply and a 2 A nominal current. A range of faults were introduced into the machine models. Figure 5, Figure 6 and Figure 7 show the variation of the state variables as functions of time.

The motor current rises very steeply on switch-on, the well-known behaviour of the three-phase induction machine. Phase 1 represents the period during which the machine runs freely; phase 2 is the transition period between no-load running and full load operation while phase 3 represents the period during which the point blade movement takes place.

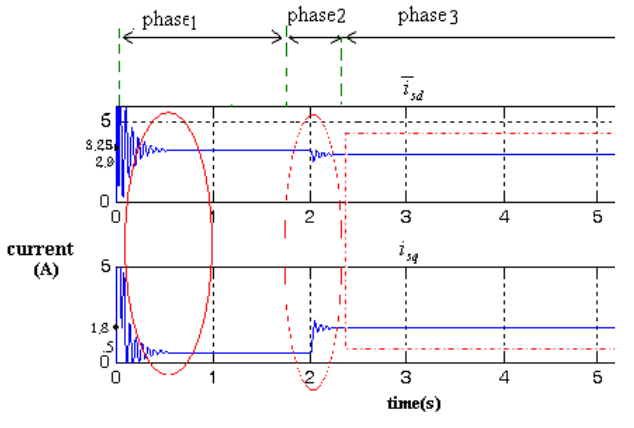

Figure 5: Potential Fault Locations in Measured State Variables

Figure 5 represents i_{sd} and i_{sq}, the stator currents, as functions of time. These were defined as X_1 and X_2 in the electric point machine model. When the behaviour of the motor changes, variations are expected in several state variables, including the stator currents. Simulated machine faults were introduced in phase 1 of the operating cycle shown in Figure 6.

Similar changes in the performance of the gear box and point blades were introduced in phases 2 and 3 of the operating cycle, respectively. The focus of the present paper is on the variations in the state variables and Kalman filter residuals that appear in phase 3 of the operating cycle, permitting close monitoring of the point blades' condition. In normal and no-fault conditions, the parameters i_{sd} and i_{sq} reach levels of 3.25 A and 0.5 A, respectively, after the switch-on oscillations have died down. These values change to 2.9 A and 1.8 A at the start of the phase 2 (after 2 seconds) of the point machine operation cycle. This is when the electric machine starts to move the blades, allowing the mechanical load to affect the machine current.

Figure 6 shows ψ_{rd}, ψ_{rq},, the rotor fluxes, estimated by the Kalman filter for the no-fault condition. These two parameters have been modelled as state variables X_3 and X_4. They cannot be measured directly and are thus determined by means of the state observer. The rotor speed ω is another variable that has been introduced in the machine model. In the no-load condition the rotor speed reaches a value of 314 rad/s while, in the loaded situation, when the machine is acting against a load of 5500 N, the speed reduces to 292 rad/s.

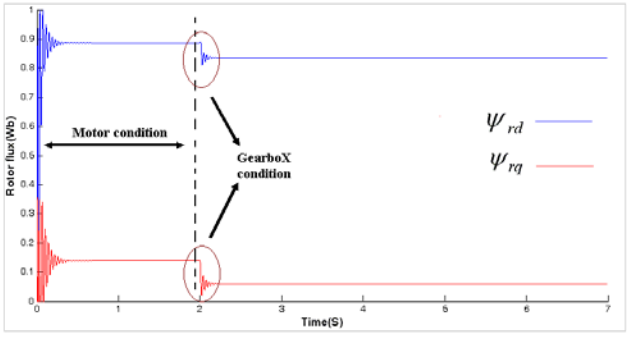

Figure 6: Estimation of State Variables (X3, X4) with Kalman Filter

Figure 7, shows the variation of this parameter for a machine operating cycle. It must be mentioned that the initial oscillations are consequences of the modelling approach used and do not represent mechanical oscillations of the drive.

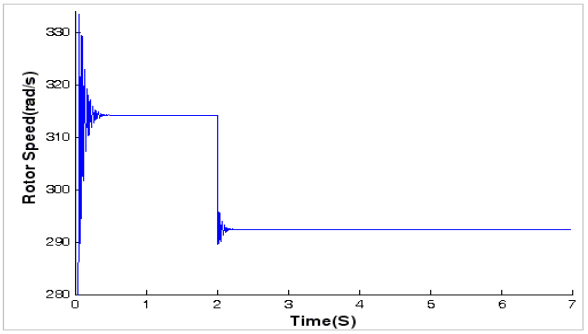

Figure 7: No Fault Rotor Speed (X5) Estimated

4.1. Point Fault Due to Dry Slide Chairs

As mentioned before, the majority of point machine failures are associated with dry slide chairs or movement of the sleepers and rails, resulting from the relatively lack of stability of ballasted track. Conventional railway points require regular adjustments to compensate for wear in point machine blades, cams, hinges of linkages and detection point machines. The slide-plates on which the points move require regular lubrication to ensure reliable low friction operation and longer life. In normal conditions, the maximum throwing force required to move the point machine blades in the normal or reverse directions is 5500 N. Due to dryness of the slide chairs, this force can increase to a value of 8000 N.

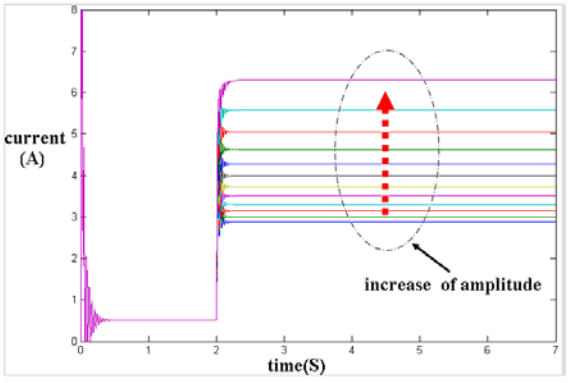

Figure 8: Stator Current of the Induction Motor of a Point Mechanism Suffering Dry Chairs

Direct measurement of this force is possible, by means of load cells. This approach has been adopted for several point condition monitoring systems. However, recognising the difficulties in installation, calibration and maintenance of the sensors in the harsh railway environment, the authors of the present paper decided to determine and analyse the forces indirectly, through estimation of the motor state variables. Their approach does not rely on a mechanical linkage to detect incipient failures in the mechanism.

Figure 8 shows the amplitude of the stator current (i_{sd}), when a dry slide chair condition occurs in the point mechanism. The steady state level of the current in phase 3 of the operation increases right from the start of the transitional phase 2 of the cycle.

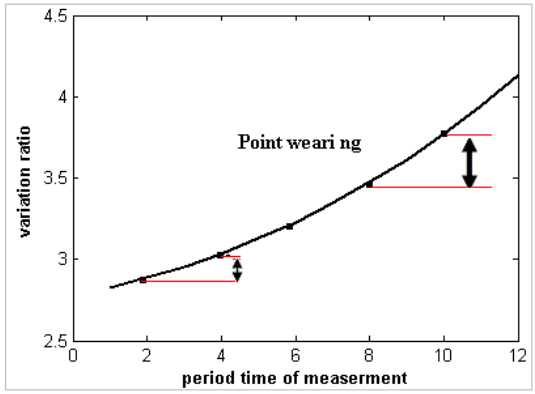

Figure 9: Change in the Current Due to a Friction Coefficient Increase

Figure 9 shows the changes in the stator current as a result of an increase in the friction coefficient in the slide chairs. As this diagram shows, the rate of increase is higher when the friction coefficient rises substantially above the normal conditions.

As the dryness rises over time, the throwing load to achieve a point movement is increased. This is directly related to the operating force.

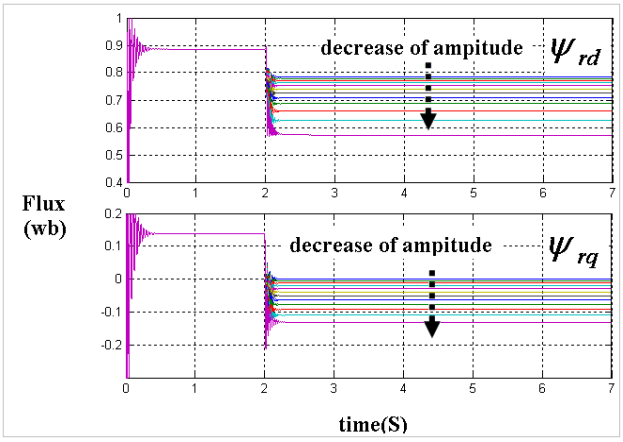

Figure 10: Induction Motor Rotor Flux of Point Mechanism in Wear Condition

Figure 10 and Figure 11 represent the variations in estimated rotor flux and speed, in a faulty condition due to point fault.

Figure 8, Figure 10 and Figure 11 are used to show the changes in the state variables due to dry slide chairs during the second phase.

The value of i_{sq} in phase 2, is increased from 2.8 A to 6.3 A and the rotor speed is reduced to 175 rad/s, compared to its original value which was 270 rad/s, where the load of point machine is increased to 7900 N.

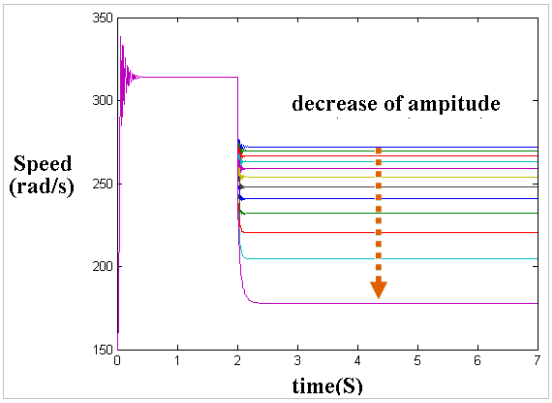

Figure 11: Variation of Speed Estimation Using Kalman Filter in Wear Condition

4.2. Failure Due to External Obstacles

Figure 12, Figure 13, and Figure 14 show that for identification of the mentioned source of failure an increase in the stator current and also a reduction in the flux and speed of the rotor from second three afterwards, should be detected.

The time of this event depends on the size of the obstacles, since a bigger obstacle causes an earlier involvement of the blades with the obstacles and so an earlier change in the machine variables.

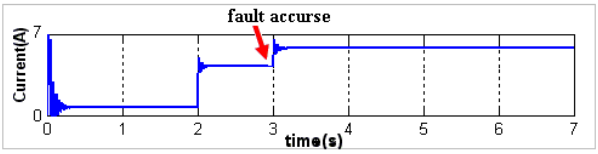

Figure 12: Increase in Stator Current Due to External Obstacles

An increase in the throwing load can be a result of different causes such as lack of lubrication, increase in friction coefficient due to changes in weather condition, inadequate point adjustments and/or existence of the obstacles between the point blade and stock rail.

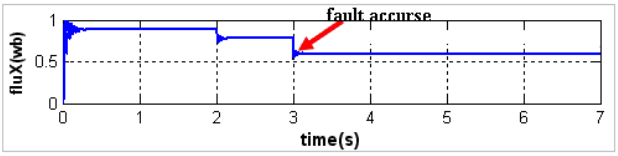

Figure 13: Decrease in Stator Flux Due to External Obstacles

The external obstacles existence can be distinguished from other causes, considering that this fault represents itself on stator current and in the latest stages of the point movement cycle.

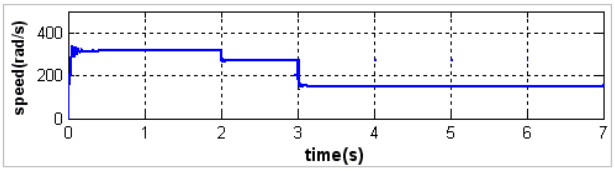

Figure 14: Reduction in Rotor Speed Due to External Obstacles

Table 2 provides a numerical comparison between different state variable values in normal and faulty conditions, which have been extracted from the above diagrams.

Table 2: Numerical Comparison of the State Variable Values in Normal and Faulty Conditions

Time	$I_{sd}(A)$	$I_{sq}(A)$	$F_{sd}(wb)$	$F_{sq}(wb)$	$W_m(rad/s)$
0<t<2	3.20	0.50	0.90	0.10	315
2<t<3	2.80	3.00	0.80	0.00	270
3<t<7	3.80	6.70	0.55	-0.14	163

The temporal behaviour of the state variables is the main parameter supporting the identification of the faults between the two above mentioned fault modes. In other words, dry slide chair will cause an increase in the stator current from the beginning of the second phase of cycle while existence of an obstacle will show its effects on the stator current from a later time, based on the size of the obstacle.

5. Conclusion

The results of the analysis represented in this paper, shows that a perfect monitoring of the point machines, using the Kalman filter state observer, is achievable. Although detection of the point machine faults, through monitoring of some variables in the system, has been the

subject of various researches before, but a reliable identification and location of the faults needed further analysis and intelligence in the monitoring systems. The algorithms proposed in this paper can provide the ability of detection and identification of the faults, using the minimum number of sensors. It is important to notice that not all alterations in the point machine variables are because of a fault in the system. For example, the machine represents higher throwing forces just after its installation and will be reduced to a normal level after some period of time. Recording and consideration of the system age and operational history can help in distinguishing the changes in the machine variables which are resulted by a fault or are due to other causes.

References

[1] Oyebande, B.O. and Renfrew, A.C., 2002. Condition monitoring of railway electric point machines. IEE Proceedings-Electric Power Applications, 149(6), pp.465-473.

[2] Márquez, F.P.G., Schmid, F. and Collado, J.C., 2003. Wear assessment employing remote condition monitoring: a case study. Wear, 255(7-12), pp.1209-1220.

[3] Velázquez, S.C., Palomares, R.A. and Segura, A.N., 2004, February. Speed estimation for an induction motor using the extended Kalman filter. In 14th International Conference on Electronics, Communications and Computers, 2004. CONIELECOMP 2004. (pp. 63-68). IEEE.

[4] Bishop, G. and Welch, G., 2001. An introduction to the kalman filter. Proc of SIGGRAPH, Course, 8(27599-23175), p.41.

[5] Wang, T., Lu, G. and Yan, P., 2019. A novel statistical time-frequency analysis for rotating machine condition monitoring. IEEE Transactions on Industrial Electronics, 67(1), pp.531-541.

[6] Isermann, R., 2005. Fault-diagnosis systems: an introduction from fault detection to fault tolerance. Springer Science & Business Media.

[7] Jin, Y., Xie, G., Li, Y., Shang, L., Hei, X., Ji, W., Han, N. and Wang, B., 2022. Multi-model train state estimation based on multi-sensor parallel fusion filtering. Accident Analysis & Prevention, 165, p.106506.

[8] Mirabadi, A., Mort, N. and Schmid, F., 1998. Fault detection and isolation in multisensor train navigation systems.

[9] Li, F. and Tang, Y., 2022. Multi-Sensor Fusion Boolean Bayesian Filtering for Stochastic Boolean Networks. IEEE Transactions on Neural Networks and Learning Systems.

[10] Shen, Y., Wang, Z., Dong, H. and Liu, H., 2022. Multi-sensor multi-rate fusion estimation for networked systems: Advances and perspectives. Information Fusion.

[11] Thongam, J.S., 2006. High Performance Sensorless Induction Motor Drive. University of Quebec at Chicoutimi, Canadá.

[12] Chen, F.C. and Khalil, H.K., 1995. Adaptive control of a class of nonlinear discrete-time systems using neural networks. IEEE Transactions on Automatic Control, 40(5), pp.791-801.

[13] Fisher, P.A. and Annaswamy, A.M., 2022. Discrete-Time Adaptive Control of a Class of Nonlinear Systems Using High-Order Tuners. arXiv preprint arXiv:2204.12634.

[14] Nguyen, P.D. and Nguyen, N.H., 2022. Adaptive control for nonlinear non-autonomous systems with unknown input disturbance. International Journal of Control, 95(12), pp.3416-3426.

[15] Maybeck, P.S., 1982. Stochastic models, estimation, and control. Academic press.

[16] Pizarro, G., Poblete, P., Droguett, G., Pereda, J. and Núñez, F., 2022. Extended Kalman Filtering for Full-State Estimation and Sensor Reduction in Modular Multilevel Converters. IEEE Transactions on Industrial Electronics, 70(2), pp.1927-1938.

[17] Yan, W., Scacchioli, A. and Rizzoni, G., 2007. Model Based Fault Diagnosis for Engine under Speed Control (No. 2007-01-0775). SAE Technical Paper.